Science of the Total Environment 473–474 (2014) 372–380

Contents lists available at ScienceDirect

Science of the Total Environment

journal homepage: www.elsevier.com/locate/scitotenv

Methodology developed to make the Quebec indoor radon potential map

Jean-Philippe Drolet [a,*], Richard Martel [a], Patrick Poulin [b], Jean-Claude Dessau [c]

[a] Institut national de la recherche scientifique, Eau Terre Environnement Research Centre (ETE-INRS), 490 de la Couronne, G1K 9A9 Quebec, Canada
[b] Institut national de santé publique du Québec (INSPQ), 945 avenue Wolfe, G1V 5B3 Quebec, Canada
[c] Agence de la santé et des services sociaux des Laurentides, 1000 rue Labelle, J7Z 5 N6 Saint-Jérome, Canada

HIGHLIGHTS

- 5 radiogeochemical datasets were used to map the geogenic indoor radon potential.
- An indoor radon potential was determined for each criterion using ANOVA.
- A combined indoor radon potential was determined and mapped.
- The radon potential based on indoor radon measurements only was mapped.
- The two maps were compared to validate the predicted geogenic radon potential.

ARTICLE INFO

Article history:
Received 25 July 2013
Received in revised form 6 December 2013
Accepted 9 December 2013
Available online 27 December 2013

Keywords:
Radon mapping
Geology
Airborne survey
ANOVA
Uranium
Sediment

ABSTRACT

This paper presents a relevant approach to predict the indoor radon potential based on the combination of the radiogeochemical data and the indoor radon measurements in the Quebec province territory (Canada). The Quebec ministry of health asked for such a map to identify the radon-prone areas to manage the risk for the population related to indoor radon exposure. Three radiogeochemical criteria including (1) equivalent uranium (eU) concentration from airborne surface gamma-ray surveys, (2) uranium concentration measurements in sediments, (3) bedrock and surficial geology were combined with 3082 basement radon concentration measurements to identify the radon-prone areas. It was shown that it is possible to determine thresholds for the three criteria that implied statistically significant different levels of radon potential using Kruskal–Wallis one way analyses of variance by ranks. The three discretized radiogeochemical datasets were combined into a total predicted radon potential that sampled 98% of the studied area. The combination process was also based on Kruskal–Wallis one way ANOVA. Four statistically significant different predicted radon potential levels were created: low, medium, high and very high. Respectively 10 and 13% of the dwellings exceed the Canadian radon guideline of 200 Bq/m^3 in low and medium predicted radon potentials. These proportions rise up to 22 and 45% respectively for high and very high predicted radon potentials.
This predictive map of indoor radon potential based on the radiogeochemical data was validated using a map of confirmed radon exposure in homes based on the basement radon measurements. It was shown that the map of predicted radon potential based on the radiogeochemical data was reliable to identify radon-prone areas even in zones where no indoor radon measurement exists.

1. Introduction

In the last decades, studies showed that radon and its decay products are carcinogenic to humans and were classed as a group 1 substance (IARC, 1988). Alpha particles emitted from radon gas and its solid decay products are the second leading cause of lung cancer after tobacco smoking (WHO, 2009). Many countries developed maps of radon-prone areas to manage the exposure of their population to high indoor radon concentrations (Alexander and Devocelle, 1997; Appleton and Miles, 2010; Apte et al., 1999; Ball and Miles, 1993; Barnet et al., 2006; Doyle et al., 1990; Gundersen and Schumann, 1996; Heincke et al., 2008; Kemski et al., 2008; Lévesque et al., 1995; Martel, 1991; Savard et al., 1998; Skeppström and Olofsson, 2006; Smethurst et al., 2008; USEPA, 1993). After Health Canada lowered the Canadian radon guideline from 800 to 200 Bq/m^3 in 2007 (Health Canada, 2007), an Action plan about radon was prepared by the Quebec intersectorial radon committee. Mapping the radon-prone areas all over the Quebec territory was one of the main objectives of this Action plan. This new tool would help public health authorities identify populations living in zones with potentially high indoor radon levels and determine uniform and integrated management strategies.

There are two distinct approaches to map radon-prone areas: 1) maps based on direct indoor radon concentrations and 2) maps

* Corresponding author.
E-mail address: jean-philippe.drolet@ete.inrs.ca (J.-P. Drolet).

0048-9697/$ – see front matter © 2013 Elsevier B.V. All rights reserved.
http://dx.doi.org/10.1016/j.scitotenv.2013.12.039

based on geological information relevant to radon (Miles, 1998). Because Quebec is a vast territory with sparsely populated regions, the indoor radon concentration coverage is not uniform. There are many areas with nonexistent or limited indoor radon measurements. Mapping the radon-prone areas for the entire province of Quebec was done by combining radiogeochemical measurements and indoor radon concentration measurements. The radiogeochemical data selected to map radon-prone areas were based on their availabilities and their redundancies in international studies: (1) equivalent uranium (eU) concentration from airborne surface gamma-ray measurements, (2) geochemistry (uranium concentration in sediment samples), and (3) geology (bedrock units and surficial deposits) (Drolet, 2011). Drolet et al. (2013) showed that there are positive proportion relationships (PPR) between the radiogeochemical measurements and the basement radon concentration measurements. They also showed that those PPR along with statistical studies are efficient to determine a radon potential based on each criterion individually.

The objective of this paper is to create a map having four different levels of radon potential (low, moderate, high and very high) based on the combination of the individual radon potentials calculated from the three above radiogeochemical criteria. The combination methodology is a statistical approach that uses Kruskal–Wallis one way analyses of variance by ranks (ANOVA). The paper also presents a validation of the thresholds set for the radiogeochemical data relevant to indoor radon levels and a combination methodology of these radiogeochemical data into a map of predicted radon potential.

2. Material and methods

2.1. Material

2.1.1. Existing methodologies to map radon-prone areas

Maps of radon-prone areas based on geological information relevant to radon have been developed in many countries and were made following different methodologies. Some use correlations between geological surveys and indoor radon concentrations (Appleton et al., 2011; Barnet et al., 2006; Chen et al., 2011; Doyle et al., 1990; Friedmann and Gröller, 2010; Garcia-Talavera et al., 2013; Gruber et al., 2013; Heincke et al., 2008; Ielsch et al., 2010; Kemski et al., 1992, 2001, 2008; Miles and Appleton, 2005; Savard et al., 1998; Smethurst et al., 2008; Verdoya et al., 2009; Wattananikorn et al., 2008). Authors set thresholds on radon-related variables (uranium concentrations in soils and rocks, equivalent uranium concentrations from gamma-ray surveys, soil gas radon measurements, percentages of dwellings that exceed the action level and building characteristics) to estimate levels of radon emission potential. Another radon potential mapping methodology is based on a multi-factor scoring system (Chen, 2009; Gundersen and Schumann, 1996; Skeppström and Olofsson, 2006; USEPA, 1993). Again, thresholds are set for radiogeochemical surveys and a scoring system is determined for each criterion. Summing the points attributed to each criterion gives a total score that is discretized into final radon potential categories. The multi-factor scoring system methodology was not applicable to map Quebec radon-prone areas because it is not effective when only one criterion is available in a territory (Chen, 2009) like it is the case in the highly populated Montréal and Laval regions where only the geology criterion is available.

2.1.2. Available datasets

The datasets are made of: (1) basement radon concentrations, (2) equivalent uranium (eU) concentrations from surface gamma-ray measurements, (3) uranium concentrations in sediments, (4) bedrock units and (5) surficial deposits. The basement radon measurements dataset totalizes 3082 data from the Quebec Ministry of Health and Social Services partners including Quebec Lung Association (QLA) (63%) and Health Canada (37%) (Fig. 1).

Positive proportion relationships were established between radiogeochemical measurements and 1417 basement radon concentration measurements conducted in Quebec (Drolet et al., 2013). Equivalent uranium concentrations from surface gamma-ray measurements, uranium concentrations interpolated from geochemical surveys and the geology criterion were discretized into statistically similar groups. Kruskal–Wallis one way ANOVA (with a p-value of 0.05) on basement radon concentrations within each class were used to calculate thresholds that indicate different levels of radon potential. Equivalent uranium concentrations from airborne surface gamma-ray measurements were discretized into three groups while uranium concentrations interpolated from geochemical surveys and the geology were discretized into two groups (Table 1).

Statistical calculations were made on basement radon concentration measurements within each group. Medians, 25th and 75th percentiles, geometric means and percentages of dwellings exceeding the three North American radon guidelines (150, 200 and 800 Bq/m^3) increase from the first to the last row of Table 1. Groups in the first row implied the lowest radon potential while those in the second row, a higher radon potential level. The gamma-ray spectrometry criterion $\geq$ 1.25 ppm has the highest radon potential. The methodology that combines the radon potential from each criterion into a total radon potential is presented herein.

2.2. Methods

2.2.1. Validation of the thresholds set for each discretized criterion

The thresholds limiting the statistically different groups were determined by calculating p-values with Kruskal–Wallis one way ANOVA by ranks. The hypothesis that the compared groups shared a common basement radon concentration mean can be rejected at the 95% confidence level when a p-value lower than 0.05 was calculated. Those p-values were calculated from the basement radon concentration dataset that included 3082 indoor radon measurements.

2.2.2. Combination of the radon potentials based on the three criteria

The information for the three radiogeochemical criteria was extracted for each of the 3082 basement radon concentration measurements using ESRI's ArcGIS 10.0 (ESRI, 2012). Table 2 shows the possible groups for the three criteria. A "No data" group was added for the airborne gamma-ray spectrometry and the geochemistry criteria because these predictors do not cover entirely the Quebec territory contrary to the geology criterion. By adding a "No data" value to the gamma-ray spectrometry and geochemistry criteria, all the three criteria have a possible value at each cell in the studied area. The size of the cells is inhomogeneous between the three criteria. The uranium concentrations in sediment dataset are made of a 100 m $\times$ 100 m grid and the bedrock unit dataset of a 40 m $\times$ 40 m grid. The eU concentrations from surface gamma-ray measurement dataset are made of multiple surveys having their grid sizes ranging from 25 m $\times$ 25 m to 1 km $\times$ 1 km. Non-dimensional values (0–1–2–N.D.) were also associated to each group as a simplification. For example, a basement radon concentration occurring in a region where there is a gamma-ray concentration of 2 ppm in equivalent uranium ("$\geq$1.25 ppm of eU" group), with non-existing interpolated geochemical data ("No data" group) and over a uranium-rich bedrock unit not confined by a silt/clay barrier ("Radon-prone units" group) was associated to non-dimensional values 2, N.D., and 1. Having four airborne gamma-ray spectrometry groups, four geochemistry groups and two geology groups, there are 32 possible scenarios. Powers of two values (2^n where n is a non-negative integer ranging from 0 to 9 herein) were also attributed to each group (Table 2). Summing the powers of two related to each scenario leads to 32 unique summations ranging from 273 to 648 (Table 3). Previous example (2–N.D.–1) could be expressed as 4–128–512 in terms of powers of two and would represent scenario 644 ($4 + 128 + 512 = 644$).

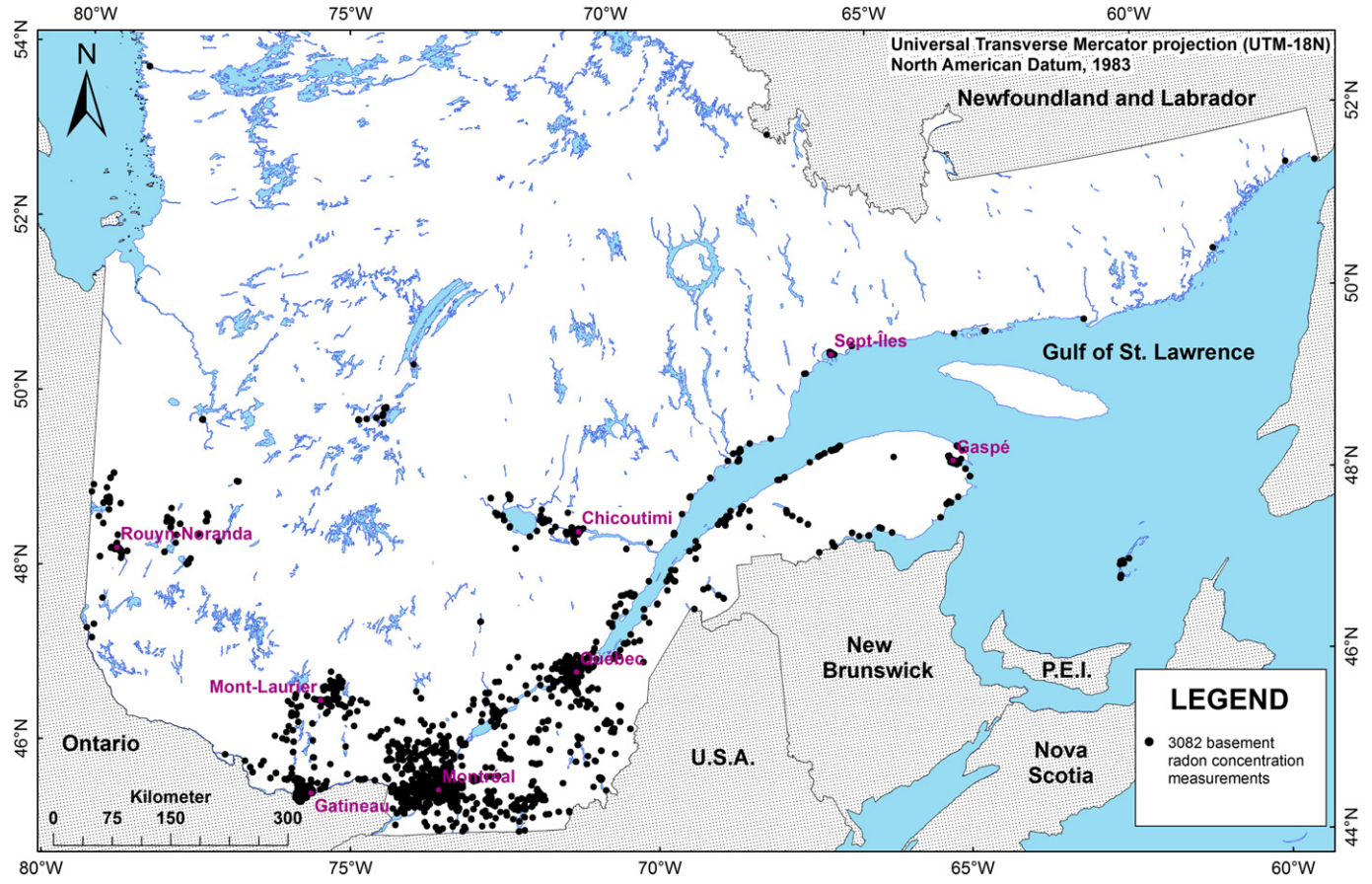

Fig. 1. Location of the basement radon concentration measurements of the Quebec dataset.

Kruskal–Wallis one way ANOVA by ranks was performed on basement radon concentrations within scenarios (Table 3) to determine if some of the scenarios were statistically similar, i.e. the basement radon concentrations within these scenarios share a common mean at the 95% confidence level. The ANOVA and p-values were calculated with SigmaStat's functions featured into SigmaPlot 12 (Systat Software Inc.). If a p-value above 0.05 was calculated when comparing two scenarios, the basement radon concentration distributions within these two scenarios were not significantly statistically different. The radon emission potential associated to these two scenarios could then be statistically similar, i.e. the exposition to a specific radon level could be statistically the same. This methodology was used to regroup statistically significant similar scenarios into groupings.

Starting with the 32 scenarios presented in Table 3, two scenarios were initially removed from the regrouping analysis (scenarios 328 and 584) because there is no basement radon measurement included in these scenarios. Regrouping analysis then started with 30 scenarios, all of them containing at least one basement radon concentration measurement.

Table 1
Discretized criteria into three (airborne gamma-ray spectrometry) or two (geochemistry and geology) statistically different groups based on the Kruskal–Wallis one way ANOVA results (from Drolet et al., 2013).

Airborne gamma-ray spectrometry (x: eU concentration in ppm)	Geochemistry (y: U concentration in ppm)	Geology
1) $x < 0.75$	$y < 20$	No uranium-rich bedrock or uranium-rich bedrock confined by a silt/clay barrier
2) $0.75 \leq x < 1.25$	$y \geq 20$	Uranium-rich bedrock not confined by a silt/clay barrier
3) $x \geq 1.25$	–	–

All scenarios were compared to scenario 273, which represents the theoretically lowest radon potential (non-dimensional values 0–0–0). The Kruskal–Wallis one way ANOVA were calculated for all pairs individually. Scenarios statistically similar to scenario 273 (p-value > 0.05) were regrouped to create grouping 1. The remaining scenarios were compared to grouping 1 and the statistically similar scenarios were included to the grouping 1.

Kruskal–Wallis one way ANOVA by ranks were performed between the scenarios not included in grouping 1 and the scenario having theoretically the highest radon potential; scenario 580 (non-dimensional values 2–2–1). Again, all pairs were analyzed individually and statistically similar scenarios were regrouped to create grouping 2. The remaining scenarios were compared to grouping 2 to merge the scenarios statistically similar to grouping 2.

Scenarios statistically similar to minimum and maximum radon potential scenarios were included in groupings at this point. Kruskal–Wallis

Table 2
Non-dimensional values and powers of two attached to each group for the three radiogeochemistry criteria. (N.D. means "No data" groups).

Radiogeochemistry criteria	Groups	Non-dimensional values	Powers of two
Gamma-ray spectrometry	<0.75 ppm of eU	0	1
	0.75 to 1.25 ppm of eU	1	2
	≥1.25 ppm of eU	2	4
	No data	N.D.	8
Geochemistry	<10 ppm of U	0	16
	10 to 20 ppm of U	1	32
	≥20 ppm of U	2	64
	No data	N.D.	128
Geology	Non radon-prone units	0	256
	Radon-prone units	1	512

Table 3
Non-dimensional values and powers of two (in parenthesis) associated to the 32 possible scenarios. The last column shows the 32 unique powers of two summations. N.D. represents the "No data" groups.

Non-dimensional values associated to gamma-ray spectrometry	Non-dimensional values associated to geochemistry	Non-dimensional values associated to geology	Powers of two summations
0 (1)	0 (16)	0 (256)	273
0 (1)	1 (32)	0 (256)	289
0 (1)	2 (64)	0 (256)	321
0 (1)	N.D. (128)	0 (256)	385
1 (2)	0 (16)	0 (256)	274
1 (2)	1 (32)	0 (256)	290
1 (2)	2 (64)	0 (256)	322
1 (2)	N.D. (128)	0 (256)	386
2 (4)	0 (16)	0 (256)	276
2 (4)	1 (32)	0 (256)	292
2 (4)	2 (64)	0 (256)	324
2 (4)	N.D. (128)	0 (256)	388
N.D. (8)	0 (16)	0 (256)	280
N.D. (8)	1 (32)	0 (256)	296
N.D. (8)	2 (64)	0 (256)	328
N.D. (8)	N.D. (128)	0 (256)	392
0 (1)	0 (16)	1 (512)	529
0 (1)	1 (32)	1 (512)	545
0 (1)	2 (64)	1 (512)	577
0 (1)	N.D. (128)	1 (512)	641
1 (2)	0 (16)	1 (512)	530
1 (2)	1 (32)	1 (512)	546
1 (2)	2 (64)	1 (512)	578
1 (2)	N.D. (128)	1 (512)	642
2 (4)	0 (16)	1 (512)	532
2 (4)	1 (32)	1 (512)	548
2 (4)	2 (64)	1 (512)	580
2 (4)	N.D. (128)	1 (512)	644
N.D. (8)	0 (16)	1 (512)	536
N.D. (8)	1 (32)	1 (512)	552
N.D. (8)	2 (64)	1 (512)	584
N.D. (8)	N.D. (128)	1 (512)	648

one way ANOVA was calculated on ungrouped scenarios to test if there was one or more statistically significant intermediate groupings.

3. Results

3.1. Validation of the thresholds set for each discretized criterion

The thresholds for the airborne gamma-ray spectrometry (Table 4) and the geology criteria (Table 5) were confirmed with the basement radon concentration dataset that includes 2098 measurements in Table 4 and 3082 measurements in Table 5.[1]

For the geochemistry criterion, an intermediate group was determined from the Kruskal–Wallis one way ANOVA results. The 1064 basement radon measurement dataset covered by the interpolated geochemical surveys and the Kruskal–Wallis one way ANOVA results show that there is three statistically significant different groups "0–10 ppm", "10–20 ppm" and "≥20 ppm" (Table 6). The three groups present an increase in the percentage of dwellings exceeding 200 Bq/m^3 and three different radon potential levels are distinguishable.

3.2. Combination of the radon potentials based on the three criteria

Scenarios statistically similar to minimum and maximum radon potential scenarios (273 and 580) were regrouped into groupings 1 and 2 based on the Kruskal–Wallis ANOVA results (Table 7).

Scenario 552 (N.D.–1–1) was included to grouping 2 because there was only one basement radon measurement associated to this scenario with a concentration of 429 Bq/m^3, which is higher than the medians of all the scenarios in this paper. Future radon measurements will help classifying this scenario in a less arbitrary way.

Also, after merging all the statistically similar scenarios to scenario 580 into the grouping 2, all the remaining scenarios at this point were compared to the grouping 2. p-Values above 0.05 were calculated from the Kruskal–Wallis one-way ANOVA between grouping 2 and scenarios 641 (0–N.D.–1) and 644 (2–N.D.–1). These scenarios were included to grouping 2. Because they are not directly statistically similar to scenario 580 (2–2–1), these scenarios (641 and 644) and scenario 552 (only 1 measurement of 429 Bq/m^3) were removed from the Kruskal–Wallis one-way ANOVA on all the scenarios included into the grouping 2 (Table 7). An asterisk was added to these three scenarios and this is why there is only 9 degrees of freedom for the calculation of the p-value in the lowest part of Table 7.

At this step, there were twenty-two scenarios included into two groupings, eight ungrouped scenarios and two scenarios excluded from the regrouping analysis due to the lack of basement radon measurements (scenarios 328 and 584). The eight remaining scenarios were all compared with a Kruskal–Wallis one-way ANOVA to test if they were all statistically similar. A p-value lower than 0.05 when comparing the eight ungrouped scenarios confirmed the presence of two or more intermediate groupings. The remaining scenarios were compared to the scenarios that have the lowest and highest median between the remaining ones (scenario 385 for the lowest median and scenario 388 for the highest median). Kruskal–Wallis one-way ANOVA results determined two intermediate groupings presented in Table 8.

All the 30 scenarios included in the regrouping analysis were grouped into one of the four groupings. A last Kruskal–Wallis one-way ANOVA was performed on the four groupings to validate the statistical homogeneity on the basement radon concentrations within each grouping and the statistical heterogeneity on the basement radon concentrations between the four groupings (Table 9). A p-value lower than 0.05 confirmed that the four groupings were statistically different.

An increase from grouping 1 to grouping 2 in the medians, 25th percentiles, 75th percentiles and percentages of dwellings that exceed the three North American radon guidelines is shown in Table 9. The radon potentials associated to these four groupings, thus, also increase. The four groupings were renamed from the radon potential level that they imply for a more convenient use in the last sections:

- Grouping 1 = Low radon potential;
- Grouping 3 = Medium radon potential;
- Grouping 4 = High radon potential;
- Grouping 2 = Very high radon potential.

The first class to present at least 20% of the dwellings exceeding 200 Bq/m^3 is grouping 4. It is a threshold in some countries, like in Norway, where such an area is considered as a high-risk zone (Strand et al., 2005). This is why the terminology "High radon potential" was associated to grouping 4. Grouping 2, which presents 45% of the dwellings exceeding 200 Bq/m^3 (more than two times the thresholds) was renamed "Very high radon potential". The first two groupings (1 and 3) do not have null radon potentials (renamed low radon potential and medium radon potential, respectively), but they are significantly lower than the last two groupings (4 and 2).

3.3. Radon potential maps

A scenario number and a radon potential were attributed to each cell based on the previous regrouping analysis results. Possible radon potential levels are low, medium, high and very high. A fifth level (unknown radon potential) was added because of the scenarios 328 and 584 that are not sampled by the actual basement radon concentration measurement dataset. Fig. 2 shows the radon potential based on the combination of the three criteria for the province of Quebec. The size of each cell in Fig. 2 is the same as the coarsest predictor used to determine its radon potential ranging from 40 m × 40 m to 1 km × 1 km.

[1] The geology criterion covers the entire territory including all the available measurements.

Table 4
Kruskal–Wallis one way ANOVA on the three confirmed groups of equivalent uranium concentration from airborne surface gamma-ray measurements. The percentages of dwellings above the three thresholds are arithmetic values.

Group (x in ppm of eU)	n	Median (Bq/m^3)	25th percentile (Bq/m^3)	75th percentile (Bq/m^3)	Geometric mean (Bq/m^3)	Geometric standard deviation (Bq/m^3)	% [Rn] ≥ 150 Bq/m^3	% [Rn] ≥ 200 Bq/m^3	% [Rn] ≥ 800 Bq/m^3
$0 < x < 0.75$	742	57	30	122	63	2.6	18.9	12.4	0.3
$0.75 \leq x < 1.25$	869	81	39	172	83	2.8	30.3	20.7	0.7
$x \geq 1.25$	487	126	59	224	117	2.8	42.3	28.7	2.5

$\chi^2 = 113.629$ with 2 degrees of freedom (p-value between three groups ≤ 0.001; statistically significant difference).

Table 5
Kruskal–Wallis one way ANOVA on the two confirmed groups of radon potential based on the geology criterion. The percentages of dwellings above the three thresholds are arithmetic values.

Group	n	Median (Bq/m^3)	25th percentile (Bq/m^3)	75th percentile (Bq/m^3)	Geometric mean (Bq/m^3)	Geometric standard deviation (Bq/m^3)	% [Rn] ≥ 150 Bq/m^3	% [Rn] ≥ 200 Bq/m^3	% [Rn] ≥ 800 Bq/m^3
Potentially low radon emission level based on geology	2470	68	33	141	70	2.7	23.2	14.7	0.7
Potentially high radon emission level based on geology	612	100	37	219	92	3.1	36.4	27.5	1.6

$\chi^2 = 31.449$ with 1 degree of freedom (p-value between two groups ≤ 0.001; statistically significant difference).

Fig. 3 shows a map of the radon potential based only on the direct 3082 basement radon measurements. This map was generated by calculating the percentage of dwellings above the Canadian radon action level of 200 Bq/m^3 for each municipality. Regional county municipality (RCM) is the county-like political entity used to create the map. It is a large political/administrative entity made of a cluster of approximately 10 to 40 municipalities. A minimum of 5 basement radon measurements per RCM was required to calculate the radon potential based on direct basement radon measurements, as suggested by Drolet et al. (2013). The same radon potential was attributed to each municipality that has at least one basement radon measurement within the RCM. In some areas where the indoor radon sampling is dense (e.g. Montréal, Québec, Gatineau and Mont-Laurier), the radon potential was calculated for each municipality and not for the entire RCM.

Comparing Figs. 2 and 3 provides the efficiency of the model at correctly predicting the radon potential. The areas confirmed to be radon-prone from the basement radon measurements (Fig. 3) were compared to the areas predicted to be radon-prone from the combination of the three radiogeochemical data (Fig. 2). The comparison is made for determining whether a municipality/RCM is radon-prone or not from the basement radon measurements (Fig. 3) and then checked against the map of the predicted radon potential (Fig. 2) whether this area was predicted to be radon-prone or not. Eq. (1) is used to calculate the efficiency:

$$\text{Efficiency}(\%) = \frac{\text{area predicted to be radon prone (or not) from the radiogeochemical data}}{\text{area confirmed to be radon prone (or not) from the basement radon measurements}} \times 100. \quad (1)$$

Table 10 shows the efficiencies of the predictions from Eq. (1).

This comparison showed that 85% of the area located in municipalities where less than 20% of the dwellings exceed 200 Bq/m^3 (green in Fig. 3) has a low or medium predicted radon potential (green or yellow in Fig. 2). For the municipalities with 20 to 40% of the dwellings above 200 Bq/m^3 (orange in Fig. 3), 32% of the area has a high or very high predicted radon potential (orange or red in Fig. 2). This percentage grows up to 41% (orange or red in Fig. 2) for the municipalities where more than 40% of the dwellings exceed the action level (red in Fig. 3).

4. Discussion

According to the results presented in Tables 7 and 8, the eU concentrations from airborne gamma-ray surveys have the biggest impact in the determination of the radon potential levels. All the scenarios that have a non-dimensional value of 2 for the gamma-ray spectrometry predictor (≥1.25 ppm of eU) are included in the very high radon potential grouping, except for scenario 388 who is in the high radon potential grouping. This predictor is strongly correlated to basement radon concentration measurements. The main problem is that the airborne gamma-ray surveys cover only 15–20% of the Quebec territory. This is the reason why this study suggests using all the three available predictors together to determine the radon potential. 98% of the studied zone has a radon potential defined by the proposed model. Such an important coverage is caused by the use of quantitative and qualitative data together to determine the radon potential. The model may cover 100% of the studied zone when the scenarios 328 and 584 will be sampled with future basement radon measurements.

The efficiency of the model to predict high indoor radon concentrations (more than 20% of the dwellings above 200 Bq/m^3) is affected by the method used to calculate it and the way the collected data are distributed. The ratio between the area predicted to be radon-prone by the radiogeochemical data approach and the area confirmed by the

Table 6
Kruskal–Wallis one way ANOVA on the three groups of uranium concentration interpolated from geochemical surveys. The percentages of dwellings above the three thresholds are arithmetic values.

Group (x in ppm)	n	Median (Bq/m^3)	25th percentile (Bq/m^3)	75th percentile (Bq/m^3)	Geometric mean (Bq/m^3)	Geometric standard deviation (Bq/m^3)	% [Rn] ≥ 150 Bq/m^3	% [Rn] ≥ 200 Bq/m^3	% [Rn] ≥ 800 Bq/m^3
$0 < x < 10$	702	66	26	143	67	2.9	23.2	16.4	0.7
$10 \leq x < 20$	260	88	41	203	93	2.9	33.1	25.8	2.7
$x \geq 20$	102	195	118	358	181	3.1	61.8	48.0	7.8

$\chi^2 = 71.743$ with 2 degrees of freedom (p-value between three groups ≤ 0.001; statistically significant difference).

Table 7
Kruskal–Wallis one-way ANOVA results on the basement radon concentrations within scenarios when comparing statistically similar scenarios to the theoretically lowest radon potential scenario (273 for grouping 1) and to the theoretically highest radon potential scenario (580 for grouping 2).

Grouping 1				
Scenario number (non–dimensional values)	n	Median (Bq/m^3)	25th percentile (Bq/m^3)	75th percentile (Bq/m^3)
273 (0–0–0)	159	44	25	93
280 (N.D.–0–0)	276	61	22	141
289 (0–1–0)	90	52	29	108
296 (N.D.–1–0)	2	61	15	106
321 (0–2–0)	8	39	16	56
392 (N.D.–N.D.–0)	444	50	26	93
529 (0–0–1)	23	41	22	118
545 (0–1–1)	4	43	15	154
577 (0–2–1)	2	15	15	15
χ^2 = 11.853 with 8 degrees of freedom (p–value=0.158; scenarios are statistically similar)				
Grouping 2				
Scenario number (non–dimensional values)	n	Median (Bq/m^3)	25th percentile (Bq/m^3)	75th percentile (Bq/m^3)
276 (2–0–0)	15	141	44	501
292 (2–1–0)	45	155	61	366
322 (1–2–0)	15	197	67	390
324 (2–2–0)	46	245	140	491
530 (1–0–1)	49	155	74	285
532 (2–0–1)	8	204	123	376
546 (1–1–1)	7	233	155	418
548 (2–1–1)	22	257	104	562
*552 (N.D.–1–1)	1	429	429	429
578 (1–2–1)	18	178	106	435
580 (2–2–1)	13	188	156	301
*641 (0–N.D.–1)	82	126	33	288
*644 (2–N.D.–1)	17	111	54	226
χ^2 = 9.898 with 9 degrees of freedom (p–value=0.359; scenarios are statistically similar)				

: Bases of comparison

Table 8
Kruskal–Wallis one-way ANOVA results on the basement radon concentrations within the two intermediate groupings.

Grouping 3				
Scenario number (non–dimensional values)	n	Median (Bq/m^3)	25th percentile (Bq/m^3)	75th percentile (Bq/m^3)
274 (1–0–0)	123	74	37	152
385 (0–N.D.–0)	374	63	33	119
386 (1–N.D.–0)	463	78	37	152
648 (N.D.–N.D.–1)	212	74	30	148
χ^2 = 4.211 with 3 degrees of freedom(p–value=0.240; scenarios are statistically similar)				
Grouping 4				
Scenario number (non–dimensional values)	n	Median (Bq/m^3)	25th percentile (Bq/m^3)	75th percentile (Bq/m^3)
290 (1–1–0)	89	89	48	159
388 (2–N.D.–0)	321	104	52	178
536 (N.D.–0–1)	49	96	28	185
642 (1–N.D.–1)	105	93	30	231
χ^2 = 1.195 with 3 degrees of freedom (p–value = 0.754; scenarios are statistically similar)				

: Bases of comparison

basement radon measurements neglects the variability of the predicted radon potential into a municipality. This fact is amplified for large suburb municipalities like Gaspé. In this large municipality (up to 1120 km^2), most of the habited zones are on the coast. This region has black shale and has a high predicted radon potential from the radiogeochemical data model. The inland uninhabited zone has a low predicted radon potential from the radiogeochemical data model because the underlying bedrocks mostly consist of sandstone, siltstone and/or limestone (Globensky, 1993). According to the basement radon measurements, more than 40% of the coastal dwellings exceed 200 Bq/m^3 in this municipality (Fig. 3) which confirms the high predicted radon potential based on the radiogeochemical data (Fig. 2). On the other hand, the inland zone is considered a radon-prone area because "more than 40% of the dwellings exceed the action level" is applied to the entire municipality. The ratio between predicted radon-prone zones and validated radon-prone zones is then lowered, and so is the calculated efficiency of the model. 36% of the area located in municipalities where more than 20% of the dwellings exceed 200 Bq/m^3 (radon-prone municipalities) has a high or very high predicted radon potential from the radiogeochemical data. Moreover, this percentage might be higher by eliminating large uninhabited zones so the model is considered efficient to predict high indoor radon concentrations.

The municipalities with less than 20% of the dwellings exceeding 200 Bq/m^3 are less affected by the contingence effect presented in this section. With 85% of the area located in these municipalities having a low or medium predicted radon potential, the model is efficient to highlight lower radon-risk zones.

This approach was used to validate the model because there were only 3082 basement radon concentration measurements available for this study. Another way to validate a model is by using a training set of data to develop the model and a validating dataset to measure its efficiency (Papadopoulou-Vrynioti et al., 2013). The power of the statistical analysis based on Kruskal–Wallis one-way ANOVA would be reduced by pulling out a validation dataset. Some scenarios would include less basement radon measurements or would not be covered.

Nonetheless, the radon potential model has some limitations. Basing a system of classification on Kruskal–Wallis one-way ANOVA that includes groups with less than 10 basement radon concentration measurements (like in Table 7) has a relatively high degree of uncertainty due to the log-normal distribution and high degree of variability associated with indoor radon measurements. Future basement radon measurements will increase the power of the statistical analysis. Also, the internal validity of the three criteria used to predict the indoor radon potential was presented by Drolet et al. (2013). Positive proportion relationships (PPR) were demonstrated between the three criteria and the basement radon concentration measurements. But uncertainties on the three criteria were also presented which create variability in the model. The external validity of the model (its capacity to be generalized to other contexts (geology, house type, climate)) was not demonstrated. One should have to use the same methodology in another province or country to do so. The thresholds set on the radon related criteria may vary and not the same three criteria may be available for a different study, but one would end up with a map having statistically significant different levels of predicted radon potential by using the methodology presented herein.

Since June 2007, the Canadian radon guideline was lowered from 800 to 200 Bq/m^3. In 2009, a radon potential map was asked by the

Table 9
Kruskal–Wallis one-way ANOVA results on the basement radon concentrations within the four groupings. The percentages of dwellings above the three thresholds are arithmetic values.

Grouping	n	Median (Bq/m^3)	25th percentile (Bq/m^3)	75th percentile (Bq/m^3)	Geometric mean (Bq/m^3)	Geometric standard deviation (Bq/m^3)	% [Rn] ≥ 150 Bq/m^3	% [Rn] ≥ 200 Bq/m^3	% [Rn] ≥ 800 Bq/m^3
Grouping 1	1008	51	25	104	55	2.6	16.0	10.2	0.5
Grouping 3	1172	70	36	139	71	2.6	22.5	13.3	0.3
Grouping 4	564	96	45	185	90	2.6	32.1	21.5	0.0
Grouping 2	338	170	74	313	156	3.1	56.2	45.0	5.3

$\chi^2 = 266.440$ with 3 degrees of freedom (p-value between four groups ≤ 0.001; statistically significant difference).

Quebec intersectorial radon committee as one of the main objectives of its Action plan about radon. The methodology presented herein furnishes a new tool that identifies radon-prone areas. More indoor radon concentration measurements are required to refine the definition of such zones. This refinement of the model would help the concerned sanitary authorities to determine their management strategies. Also, the radon potential map suggests some zones where there are more dwellings above the Canadian radon guideline. The sanitary authorities may use the radon potential map to promote indoor radon measurements and mitigation measures to their populations. Nonetheless, the Quebec Ministry of Health and Social Services suggests to citizens that the only safe way to know the level of radon exposure in a dwelling is to measure it, regardless of its location in the radon potential map.

5. Conclusion

Combining the three radiogeochemical criteria relevant to indoor radon concentrations into scenarios and then into total predictive radon potentials is currently the most effective way to map radon-prone areas due to the small number of available basement radon concentration measurements. The PPR (positive proportion relationships) between basement radon concentration measurements and three radiogeochemical criteria were validated. The methodology combined the radiogeochemical information into scenarios and merged statistically similar scenarios from the Kruskal–Wallis one way ANOVA results. The merged scenarios were converted into predicted radon potential levels. It allows to develop a map of predicted radon potential on almost the entire studied zone (98%) compared to the map of confirmed radon potential based on the basement radon measurements which sampled approximately 15% of the studied zone. Future basement radon measurements will refine the scenario classification and the model may evolve. Zones where scenarios 328 and 584 occur would likely be sampled by future basement radon measurements to determine their radon potential because it is presently unknown. Also, new gamma-ray surveys and/or uranium concentration measurements in sediments may modify the classification of some scenarios that has a "No data" classification. Also, the radon surveys from the petroleum industry may be used to confirm the emission level of the geological units. The existing combined map of the radon potential is the best currently available means for predicting low and high radon concentrations in

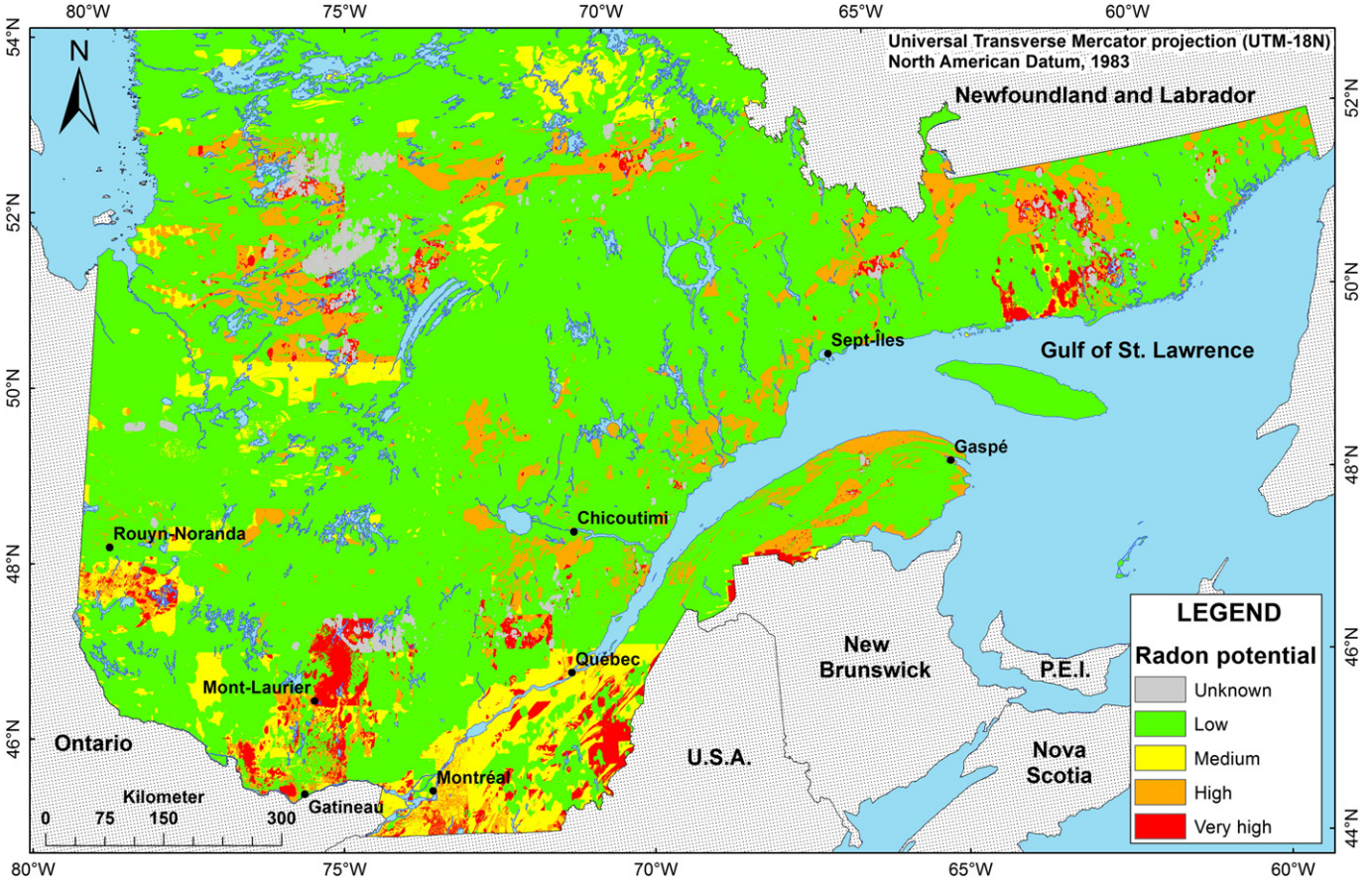

Fig. 2. Quebec predicted radon potential based on the combination of the radon potentials from the available radiogeochemical data.

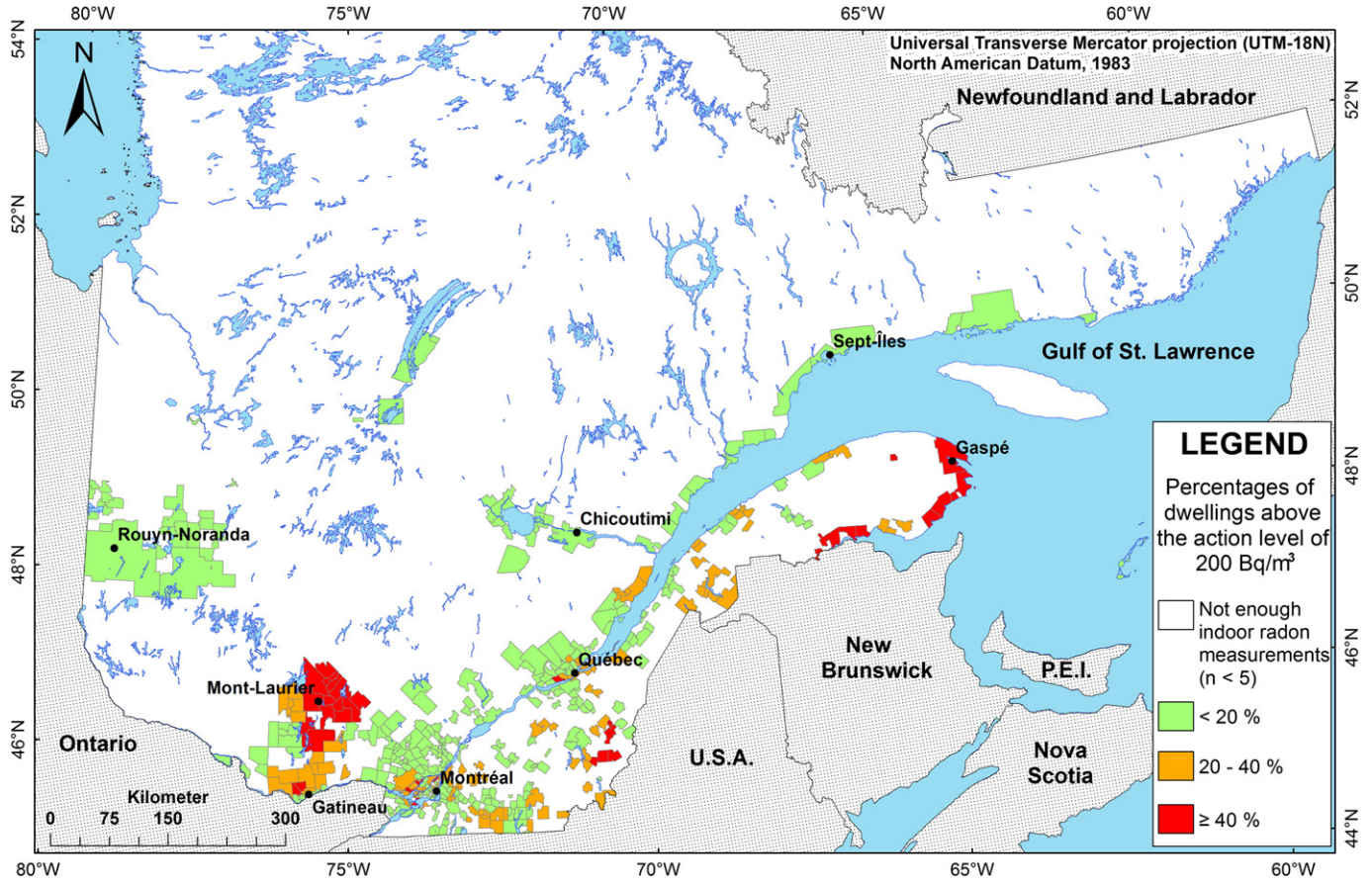

Fig. 3. Quebec radon potential based only on the 3082 basement radon measurements.

Table 10
Efficiency of the predicted radon potential based on the radiogeochemical data for the three classes of municipalities. Classification of the municipalities is based on the percentage of the dwellings that exceed the action level of 200 Bq/m^3 within their boundaries.

Classified municipalities based on the percentages of the dwellings that exceed 200 Bq/m^3	Total area (km^2)	Area predicted to be non-radon prone from the radiogeochemical data (green or yellow in Fig. 2) in the specified municipalities (km^2)	Area predicted to be radon prone from the radiogeochemical data (orange or red in Fig. 2) in the specified municipalities (km^2)	Efficiency (%)
Less than 20% of the dwellings exceed 200 Bq/m^3 (confirmed to be non-radon prone from the basement radon measurements; green in Fig. 3)	59,848	50,964		$\frac{50964}{59848} = 85\%$
Between 20 and 40% of the dwellings exceed 200 Bq/m^3 (confirmed to be radon prone from the basement radon measurements; orange in Fig. 3)	15,363		4886	$\frac{4886}{15363} = 32\%$
More than 40% of the dwellings exceed 200 Bq/m^3 (confirmed to be radon prone from the basement radon measurements; red in Fig. 3)	10,322		4257	$\frac{4257}{10322} = 41\%$

Quebec. Public health authorities may use it to promote indoor radon measurements and mitigation actions in high risk zones to protect the Quebec population against radon-related lung cancer.

Conflict of interest

No conflict of interest with other people/organizations.

Acknowledgments

The authors would like to thank the Quebec Ministère de la Santé et des Services sociaux (MSSS) for funding this research. They also gratefully acknowledge Professor André St-Hilaire (INRS-ETE) and Suzanne Gingras (INSPQ) for their inputs on the statistical analysis and the two reviewers for their precious recommendations.

References

Alexander WG, Devocelle LL. Mapping indoor radon potential using geology and soil permeability. 1997 International Radon Symposium; 1997.
Appleton JD, Miles JCH. A statistical evaluation of the geogenic controls on indoor radon concentrations and radon risk. J Environ Radioact 2010;101:799–803.
Appleton JD, Miles JCH, Young M. Comparison of Northern Ireland radon maps based on indoor radon measurements and geology with maps derived by predictive modeling of airborne radiometric and ground permeability data. Sci Total Environ 2011;409:1572–83.
Apte MG, Price PN, Nero AV, Revzan KL. Predicting New Hampshire indoor radon concentrations from geologic information and other covariates. Environ Geol 1999;37:181–94.
Ball TK, Miles JCH. Geological and geochemical factors affecting the radon concentration in homes in Cornwall and Devon, UK. Environ Geochem Health 1993;15:27–36.

Barnet I, Neznal M, Klingel R. Possible ways to radon map of Europe —from input data to result. In: Barnet I, Neznel M, Pacherova P, editors. Proceedings of the 8th international workshop on the geological aspects of radon risk mapping; 2006. p. 11–20.
Chen J. A preliminary design of a radon potential map for Canada: a multi-tier approach. Environ Earth Sci 2009;59:775–82.
Chen J, Ford K, Whyte J, Bush K, Moir D, Cornett J. Achievements and current activities of the Canadian radon program. Radiat Prot Dosimetry 2011;146: 14–8.
Doyle PJ, Grasty RL, Charbonneau BW. Predicting geographic variations in indoor radon using airborne gamma-ray spectrometry. Geological Survey of Canada, Current Research, Part A, Paper, 90-1A; 199027–32.
Drolet JP. Revue des données géoscientifiques existantes pour identifier les zones potentielles à la présence de radon domiciliaire au Québec, Canada. Université du Québec (ETE-INRS); 2011 [Master thesis, 263 pp.].
Drolet JP, Martel R, Poulin P, Dessau JC, Lavoie D, Parent M, et al. An approach to define potential radon emission level maps using indoor radon concentration measurements and radiogeochemical data positive proportion relationships. J Environ Radioact 2013;124:57–67.
Environmental Systems Research Institute (ESRI). ArcMap 10.1. Redlands, CA: ESRI; 2012.
Friedmann H, Gröller J. An approach to improve the Austrian radon potential map by Bayesian statistics. J Environ Radioact 2010;101:804–8.
Garcia-Talavera M, Garcia-Perez A, Rey C, Ramos L. Mapping radon-prone areas using γ-radiation dose rate and geological information. J Radiol Prot 2013;33: 605–20.
Globensky Y. Lexique stratigraphique canadien. Volume V-B: région des Appalaches, des basses-terres du Saint-Laurent et des Îles de la Madeleine. Gouvernement du Québec, Ministère de l'Énergie et des Ressources et Direction générale de l'exploration géologique et minérale; 1993 [327 p., DV 91–23].
Gruber V, Bossew P, De Cort M, Tollefsen T. The European map of the geogenic radon potential. J Radiol Prot 2013;33:51–60.
Gundersen LCS, Schumann RR. Mapping the radon potential of the United States: examples from the Appalachians. Environ Int 1996;22:S829–37.
Health Canada. Radon: what you need to know. Information sheet. HC Publication 4928; 2007 [4 pp.].
Heincke BH, Smethurst MA, Bjørlykke A, Dahlgren S, Rønning JS, Mogaard JO. Airborne gamma-ray spectrometer mapping for relating indoor radon concentrations to geological parameters in the Fen region, southeast Norway. In: Slagstad T, editor. Geology for Society, 11. Geological Survey of Norway, Special Publication; 2008. p. 131–43.
Ielsch G, Cushing ME, Combes P, Cuney M. Mapping of the geogenic radon potential in France to improve radon risk management: methodology and first application to region Bourgogne. J Environ Radioact 2010;101:813–20.
International Agency for Research on Cancer (IARC). Monographs on the evaluation of carcinogenic risks to humans. Man-made mineral fibres and radon, vol. 43. Lyon: IARC; 1988.
Kemski J, Klingel R, Schneider H, Siehl A, Wiegand J. Geological structure and geochemistry controlling radon in soil gas. Radiat Prot Dosimetry 1992;45:235–9.
Kemski J, Siehl A, Stegemann R, Valdivia-Manchego M. Mapping the geogenic radon potential in Germany. Sci Total Environ 2001;272:217–30.
Kemski J, Klingel R, Siehl A, Valdivia-Manchego M. From radon hazard to risk prediction-based on geological maps, soil gas and indoor measurements in Germany. Environ Geol 2008;56:1269–79.
Lévesque B, Gauvin D, McGregor RG, Martel R, Gingras S, Dontigny A, et al. Étude d'exposition au radon-222 dans les résidences de la province de Québec. Centre de santé publique de Québec; 1995 [46 pp.].
Martel R. Zones proposées pour l'échantillonage du radon dans les habitations québécoises. Ministère de l'environnement du Québec, Direction des écosystèmes urbains, Division des eaux souterraines; 1991 [77 pp.].
Miles J. Development of maps of radon-prone areas using radon measurements in houses. J Hazard Mater 1998;61:53–8.
Miles JCH, Appleton JD. Mapping variation in radon potential both between and within geological units. J Radiol Prot 2005;25:257–76.
Papadopoulou-Vrynioti K, Bathrellos GD, Skilodimou HD, Kaviris G, Makropoulos K. Karst collapse susceptibility mapping considering peak ground acceleration in a rapidly growing urban area. Eng Geol 2013;158:77–88.
Savard M, Dessau JC, Pellerin E. Le radon à oka - Rapport d'intervention de santé publique. Régie régionale de la santé et des services sociaux des Laurentides, Direction de la santé publique; 1998 [146 pp.].
Skeppström K, Olofsson B. A prediction method for radon in groundwater using GIS and multivariate statistics. Sci Total Environ 2006;367:666–80.
Smethurst MA, Strand T, Sundal AV, Rudjord AL. Large-scale radon hazard evaluation in the Oslofjord region of Norway utilizing indoor radon concentrations, airborne gamma ray spectrometry and geological mapping. Sci Total Environ 2008;407:379–93.
Strand T, Jensen CL, Ånestad K, Ruden L, Ramberg GB. High radon areas in Norway. Int Congr Ser 2005;1276:212–4.
US Environmental Protection Agency (USEPA). EPA's map of radon zones —national summary. 402-R-93-071; 1993.
Verdoya M, Chiozzi P, De Felice P, Pasquale V, Bochiolo M, Genovesi I. Natural gamma-ray spectrometry as a tool for radiation dose and radon hazard modeling. Appl Radiat Isot 2009;67:964–8.
Wattananikorn K, Emharuthai S, Wanaphongse P. A feasibility study of geogenic indoor radon mapping from airborne radiometric survey in northern Thailand. Radiat Meas 2008;43:85–90.
World Health Organization (WHO). Fact sheet no 291: radon and cancer. Available at: http://www.who.int/mediacentre/factsheets/fs291/en/, 2009. [Accessed July 17 2012].